AMERICAN SOCIETY FOR MICROBIOLOGY | Journal of Bacteriology®

RESEARCH ARTICLE

The Lipoprotein NlpE Is a Cpx Sensor That Serves as a Sentinel for Protein Sorting and Folding Defects in the *Escherichia coli* Envelope

Antoine Delhaye,[a,b] Géraldine Laloux,[a] Jean-François Collet[a,b]

[a]de Duve Institute, Université Catholique de Louvain, Brussels, Belgium
[b]WELBIO, Brussels, Belgium

ABSTRACT The envelope of Gram-negative bacteria is a complex compartment that is essential for viability. To ensure survival of the bacterial cells in fluctuating environments, several signal transduction systems, called envelope stress response systems (ESRSs), exist to monitor envelope biogenesis and homeostasis. The Cpx two-component system is an extensively studied ESRS in *Escherichia coli* that is active during exposure to a vast array of stresses and protects the envelope under those harmful circumstances. Overproduction of NlpE, a two-domain outer membrane lipoprotein of unclear function, has been used in numerous studies as a molecular trigger to turn on the system artificially. However, the mechanism of Cpx activation by NlpE, as well as its physiological relevance, awaited further investigation. In this paper, we provide novel insights into the role played by NlpE in the Cpx system. We found that, among all outer membrane lipoproteins in *E. coli*, NlpE is sufficient to induce Cpx when lipoprotein trafficking is perturbed. Under such conditions, fitness is increased by the presence of NlpE. Moreover, we show that NlpE, through its N-terminal domain, physically interacts with the Cpx sensor kinase CpxA. Our data suggest that NlpE also serves to activate the Cpx system during oxidative folding defects in the periplasm and that its C-terminal domain is involved in the sensing mechanism. Overall, our data demonstrate that NlpE acts as a sentinel for two important envelope biogenesis processes, namely, lipoprotein sorting and oxidative folding, and they further establish NlpE as a bona fide member of the Cpx two-component system.

IMPORTANCE Bacteria rely on a sophisticated envelope to shield them against challenging environmental conditions and therefore need to ensure correct envelope assembly and integrity. A major signaling pathway that performs this role in Gram-negative species is the Cpx system. An outer membrane lipoprotein of unclear function, NlpE, has long been exploited as a research tool to study Cpx in *E. coli*, since it triggers this system when overproduced or mislocalized; however, the mechanism and physiological relevance of the NlpE-Cpx connection have awaited further investigation. We elucidate a new function for NlpE by showing that it physically interacts with the Cpx sensor CpxA and acts as a sentinel that specifically monitors two essential envelope biogenesis processes, namely, lipoprotein sorting and oxidative folding.

KEYWORDS Cpx stress response, *Escherichia coli*, NlpE, cell envelope, envelope biogenesis, lipoproteins, two-component regulatory systems

The envelope of Gram-negative bacteria is a three-layer compartment composed of two membranes (i.e., the inner membrane [IM] and the outer membrane [OM]) surrounding a soluble chamber (i.e., the periplasm) in which lies the peptidoglycan

Citation Delhaye A, Laloux G, Collet J-F. 2019. The lipoprotein NlpE is a Cpx sensor that serves as a sentinel for protein sorting and folding defects in the *Escherichia coli* envelope. J Bacteriol 201:e00611-18. https://doi.org/10.1128/JB.00611-18.

Editor Yves V. Brun, Université de Montréal

Address correspondence to Géraldine Laloux, geraldine.laloux@uclouvain.be, or Jean-François Collet, jfcollet@uclouvain.be.

A.D. and G.L. are co-first authors.

Received 10 October 2018
Accepted 1 March 2019
Accepted manuscript posted online 4 March 2019
Published 24 April 2019

layer (1). At the interface between the environment and the intracellular space, the envelope hosts essential processes, including cell wall synthesis and remodeling (2), lipoprotein sorting (3), protein folding (4), and lipopolysaccharide export (5). These processes must be tightly regulated to ensure proper growth and survival of the cell. Consequently, several envelope stress response systems (ESRSs) exist to monitor their functioning and to ensure adequate repair should one of them be compromised (6, 7). A major ESRS in *Escherichia coli* and other gammaproteobacteria is the Cpx two-component system, which transduces envelope stress signals across the IM (8, 9). Under stress, the transmembrane histidine kinase CpxA autophosphorylates and transfers its phosphoryl group to the response regulator CpxR in the cytoplasm, which then binds DNA to regulate the expression of a large set of genes (10, 11). The mechanism that triggers CpxA phosphorylation is still poorly understood and probably is complex. Indeed, a large number of cues from all envelope layers, such as accumulation of misfolded proteins in the periplasm, surface attachment, IM stress due to protein imbalance, defects in lipoprotein sorting between the IM and the OM, and cell wall perturbations, have been reported to elicit a Cpx response (reviewed in reference 12).

The Cpx system can also be activated by artificial overproduction of NlpE (13), an OM-anchored lipoprotein that has been proposed to play a role in Cpx activation upon surface attachment (14, 15). Because of this property, NlpE overproduction has served over the years as a molecular trigger for the exploration of Cpx and the characterization of its regulon (8). The findings that overproduced NlpE accumulates at the IM and that retargeting of NlpE to the IM also produces a strong Cpx response (16) suggest that activation of the system results from direct or indirect interactions between NlpE and the IM Cpx sensor kinase CpxA. However, the mechanism by which NlpE turns on Cpx and the physiological relevance of this activation have remained elusive. Interestingly, the modulation of a two-component system by a remote lipoprotein is the hallmark of another major ESRS, the Rcs phosphorelay, which mostly monitors OM and cell wall damage via the OM lipoprotein RcsF (17). Whereas most Rcs-inducing cues absolutely rely on RcsF (reviewed in references 12 and 17), unambiguous data for NlpE-dependent activation of the Cpx response were missing. Recent data reported by Grabowicz and Silhavy showed that the presence of NlpE increased fitness under conditions of impaired lipoprotein trafficking, suggesting that NlpE acts as a sensor monitoring lipoprotein maturation for the Cpx system (18), although no direct evidence showing that NlpE indeed triggered Cpx under those conditions was provided. Therefore, the actual role of this lipoprotein in the cell has remained unclear.

In this work, we set out to investigate the relationship between NlpE and Cpx. First, we provide direct evidence that the Cpx system is specifically induced by NlpE when lipoprotein trafficking to the OM is compromised. Moreover, we discovered that oxidative folding defects turn on Cpx in a NlpE-dependent manner. In addition, we show that NlpE triggers Cpx by interacting, via its N-terminal domain, with the IM histidine kinase CpxA; we found that the cysteine residues located in the C-terminal domain of NlpE play a role in the redox-sensing mechanism. Together, our data further establish NlpE as a bona fide Cpx member and support the idea that NlpE acts as a Cpx sentinel for two important envelope biogenesis processes, namely, lipoprotein sorting and oxidative folding, thus providing important insights into the function of NlpE in the *E. coli* envelope.

RESULTS

NlpE activates Cpx when lipoprotein trafficking is impaired. We and others reported that rerouting NlpE to the IM constitutively triggers Cpx (16, 19) (Fig. 1A). Moreover, small amounts of an IM-targeted variant of NlpE ($NlpE_{IM}$) are sufficient to turn on *lacZ* expression from P*cpxP* (a reliable reporter for Cpx activity [9, 10]) to levels higher than those observed upon overproduction of wild-type NlpE (see Fig. S1A in the supplemental material), suggesting that the Cpx system is highly sensitive to the localization of this lipoprotein (the localization of $NlpE_{IM}$ in the IM was verified previously [16]). However, it remained to be determined whether lipoproteins other than

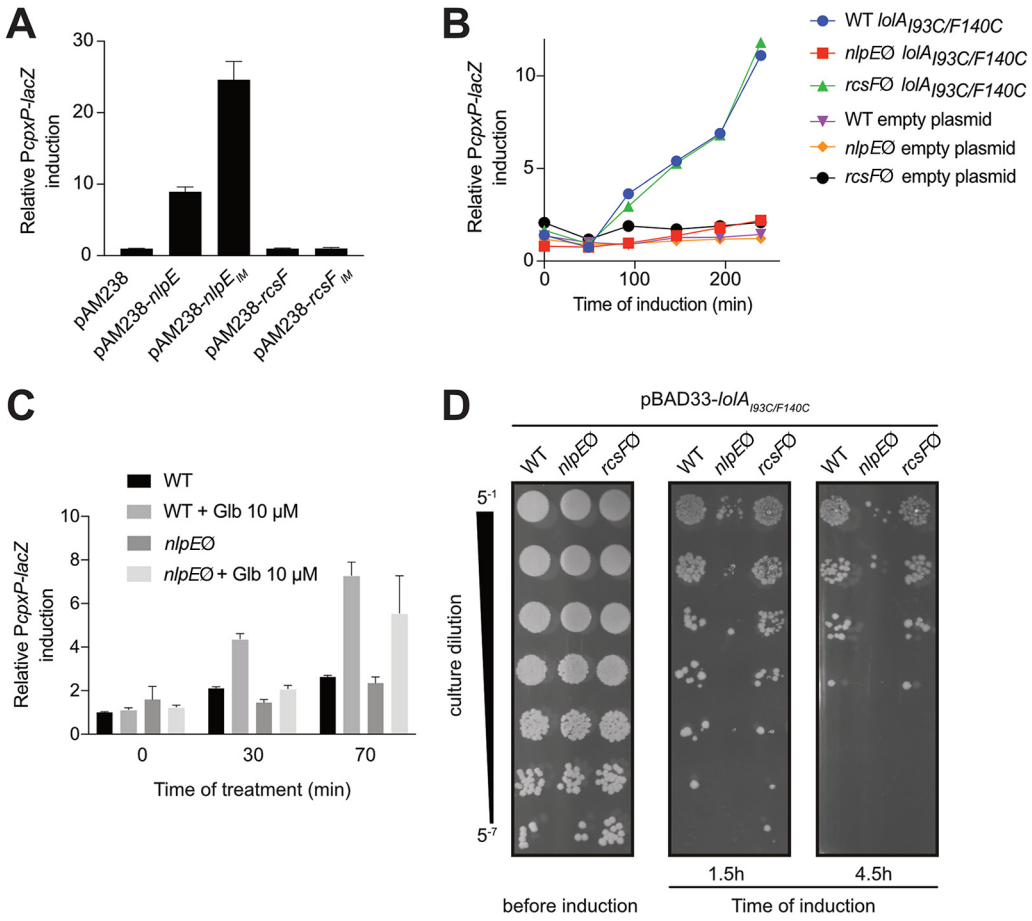

FIG 1 NlpE turns on the Cpx system and provides a fitness advantage when lipoprotein sorting is defective. (A) Overproducing and mislocalizing NlpE but not RcsF to the IM induces *lacZ* expression from the specific CpxR activity reporter P*cpxP*. The β-galactosidase activity of strains expressing wild-type *nlpE* (GL60), $nlpE_{IM}$ (GL97), wild-type *rcsF* (GL245), or $rcsF_{IM}$ (GL285) or carrying the empty pAM238 plasmid (GL61) was measured. All values were normalized to the average activity obtained for the GL61 strain. Bars represent the averages of normalized values for at least three independent clones. Error bars indicate standard deviations. (B) Inducing the expression of the dominant negative mutant $lolA_{I93C/F140C}$ from the pBAD33 plasmid leads to NlpE-dependent and RcsF-independent Cpx activation. Wild-type (WT), *nlpE*::*kanR* (*nlpEØ*), or *rcsF*::*kanR* (*rcsFØ*) cells expressing $lolA_{I93C/F140C}$ (strains AD34, AD35, and AD54, respectively) or carrying the empty pBAD33 plasmid (strains GL442, AD57, and AD173, respectively) were grown with 0.2% L-arabinose. β-Galactosidase activity from P*cpxP-lacZ* was measured every 50 min. All values were normalized to the average activity obtained for AD57 after 150 min of growth. This graph is representative of at least three independent measurements. (C) Treatment with globomycin (Glb) also leads to NlpE-dependent activation of the Cpx system. Wild-type (strain GL43) and *nlpE*::*kanR* (strain GL44) cells were grown for 150 min and then treated with 10 μM globomycin (Sigma), after which β-galactosidase activity from P*cpxP-lacZ* was measured periodically. All values were normalized to the average activity obtained for untreated GL43 cells before treatment. Bars represent the averages of normalized values from three independent clones. Error bars indicate standard deviations. (D) NlpE provides a fitness advantage when lipoprotein sorting defects occur. The $lolA_{I93C/F140C}$ gene was expressed from the pBAD33 plasmid in wild-type, *nlpE*::*kanR*, and *rcsF*::*kanR* cells (strains AD34, AD35 and AD54, respectively) before serial dilution as indicated and spotting on LB agar. This image is representative of at least three independent replicates.

NlpE can activate Cpx when their trafficking to the OM is perturbed. Thus, to investigate the specificity of the Cpx response to NlpE, we first tested the impact of rerouting the lipoprotein RcsF to the IM ($RcsF_{IM}$) on Cpx activity. RcsF is an OM lipoprotein that activates another ESRS, Rcs, when perturbations in the OM or the peptidoglycan occur (20, 21). We verified that RcsF and $RcsF_{IM}$ were produced at similar levels and were correctly localized (Fig. S1C and D). Interestingly, whereas targeting RcsF to the IM was previously reported to induce Rcs (20), no Cpx activation was observed (Fig. 1A). We next sought to address the question of the specificity of Cpx activation by NlpE by using more-global approaches. In *E. coli*, lipoprotein transport is orchestrated by the essential Lol machinery (22). In the IM, lipoproteins destined for the OM are recognized by the

ABC transporter LolCDE complex and extracted from the membrane (23). They bind the soluble chaperone LolA for transport across the periplasm (24) and then are inserted into the OM through an unknown mechanism that involves the lipoprotein LolB (25). To test whether accumulation of lipoproteins other than NlpE in the IM induced Cpx, we first used a mutant version of LolA ($LolA_{I93C/F140C}$) that strongly binds to LolCDE, thereby preventing the release of lipoproteins to the periplasm (26). Expression of $lolA_{I93C/F140C}$ activated Cpx in wild-type cells, as shown previously (26), and as expected when NlpE accumulates in the IM. Strikingly, however, these cells could not activate Cpx in the absence of NlpE (Fig. 1B). Similarly, expression of $lolA_{I93C/F140C}$ induced Rcs in wild-type cells but not in cells lacking RcsF (27) (Fig. S1B). Interestingly, the absence of NlpE had no effect on Rcs activation, while the absence of RcsF did not modulate the Cpx response in the presence of the $LolA_{I93C/F140C}$ dominant negative mutant (Fig. 1B; also see Fig. S1B), hinting at specific connections between these lipoproteins and their cognate ESRSs. Similar results were then obtained by perturbing lipoprotein trafficking with globomycin, an inhibitor of the type II Lsp signal peptidase that blocks lipoprotein maturation and thereby causes the retention of OM lipoproteins in the IM (28). Consistent with data obtained with the $LolA_{I93C/F140C}$ mutant, Cpx activation was observed in wild-type cells that had been treated for 30 min with globomycin (Fig. 1C) but not in the *nlpE* null mutant, although this difference was less pronounced at a later time point (Fig. 1C; also see Discussion). We conclude from these experiments that Cpx is specifically activated by NlpE when lipoprotein transport to the OM is perturbed.

Cpx induction by NlpE is beneficial to cells with perturbations in lipoprotein transport. The fact that NlpE activates Cpx when the transport of lipoproteins to the OM is disrupted suggests that Cpx activation may provide a fitness advantage under these conditions. To test this, we compared the abilities of wild-type and *nlpE* null cells to cope with the toxic expression of $lolA_{I93C/F140C}$. Supporting our hypothesis, we consistently observed better survival of wild-type cells than *nlpE* null cells (Fig. 1D). In contrast, preventing Rcs activation by deleting *rcsF* did not have any impact on cell survival (Fig. 1D), indicating that Cpx plays a more important role than Rcs in allowing the cells to adapt to perturbations in lipoprotein trafficking, in agreement with results reported by Grabowicz and Silhavy (18). Cells lacking the ability to activate Cpx (*cpxR* null), as well as cells lacking both *cpxR* and *nlpE*, showed reduced fitness similar to that of cells lacking *nlpE* only (Fig. S2A). Interestingly, complementation by plasmidic expression of *nlpE* not only rescued the *nlpE* null phenotype but also improved growth, compared to wild-type cells harboring an empty plasmid (Fig. S2B). This was not the case when *nlpE* was expressed in a *cpxR* null background, indicating that the fitness advantage provided by NlpE during lipoprotein sorting defects involves Cpx activation.

The N-terminal domain of NlpE activates Cpx. We next sought to obtain molecular insights into the mechanism by which NlpE induces Cpx. The lipoprotein NlpE consists of two structural domains, each folding into a β-barrel (Fig. 2A) (29). While the N-terminal domain is homologous to the lipocalin Blc, a bacterial lipoprotein that binds hydrophobic ligands (30), the C-terminal domain adopts an oligonucleotide/oligosaccharide-binding (OB) fold (31). Overproduction of NlpE has been reported to induce Cpx expression (13), probably because NlpE accumulates in the IM when its levels are increased (16). Thus, to determine whether the two domains of NlpE are required for Cpx activation, we tested the impact of overproducing the N- and C-terminal domains ($NlpE_{Nterm}$ and $NlpE_{Cterm}$) separately on Cpx activity (Fig. 2A). We verified that $NlpE_{Nterm}$ and $NlpE_{Cterm}$ were produced at similar levels (Fig. S1C). Interestingly, whereas $NlpE_{Cterm}$ in cells lacking native *nlpE* did not induce Cpx, $NlpE_{Nterm}$ alone caused Cpx induction that was comparable to that observed when full-length NlpE was expressed from the same plasmid (Fig. 2B). Furthermore, when rerouted to the IM, $NlpE_{Nterm}$ [$NlpE_{Nterm(IM)}$] but not $NlpE_{Cterm}$ [$NlpE_{Cterm(IM)}$] activated Cpx better than the corresponding OM variant (Fig. 2B), mimicking the behavior of the full-length protein (Fig. 1A). The expression levels and membrane localization of these constructs

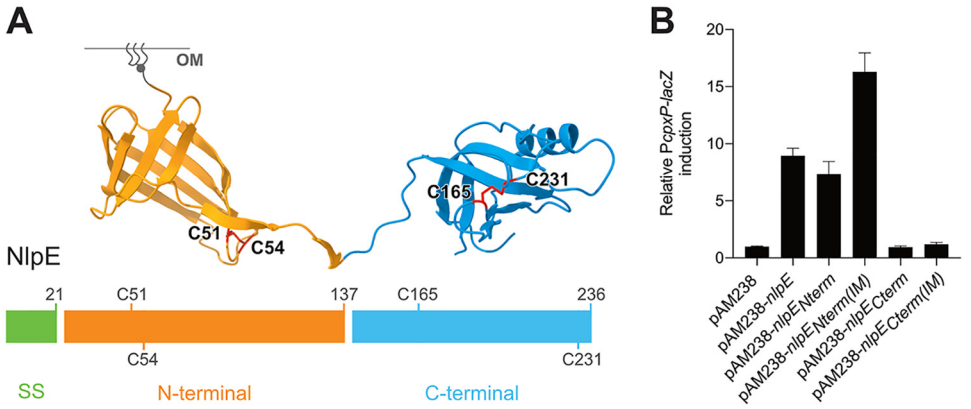

FIG 2 The N-terminal domain of NlpE is the Cpx-activating domain. (A) NlpE is composed of two structurally distinct domains. The domains were determined empirically using phylogenetic data comparing bacterial species harboring a full-length or N-terminus-only version of NlpE. We define the N-terminal domain as residues 22 to 137 (inclusive) and the C-terminal domain as residues 138 to 236 (inclusive), as indicated. The C-terminal domain was constructed by removing the sequence encoding residues 24 to 137. Disulfide bonds are drawn in red on the structure, and the corresponding cysteine residues are also shown on the one-dimensional schematics of the NlpE sequence. The lipid anchor is schematically represented in gray. SS, signal sequence for secretion. (B) The N-terminal domain of NlpE activates Cpx. β-Galactosidase activity from P*cpxP-lacZ* was measured in wild-type cells carrying the empty pAM238 plasmid (GL61) or expressing full-length *nlpE* (GL60), $nlpE_{Nterm}$ (AD171), $nlpE_{Cterm}$ (AD172), $nlpE_{Nterm(IM)}$ (AD165), or $nlpE_{Cterm(IM)}$ (AD187) from the same plasmid. All values were normalized to the average activity obtained for GL61. Bars represent the averages of normalized values from at least three independent clones. Error bars indicate standard deviations.

were verified (Fig. S1C and D). Thus, these results allow us to conclude that the N-terminal domain of NlpE plays a crucial role in controlling Cpx activation.

NlpE physically interacts with the sensor histidine kinase CpxA. How NlpE triggers Cpx when overproduced or rerouted to the IM remained unknown. A likely hypothesis was that NlpE induces Cpx by interacting with the histidine kinase CpxA, an IM protein with a large periplasmic sensor domain (32) (Fig. 3A). To investigate this, the periplasmic domain of CpxA ($CpxA_{peri}$, ~15 kDa), fused to an N-terminal Strep-tag, was coexpressed in the periplasm with NlpE. After Strep-tag pulldown, NlpE was found to coelute with $CpxA_{peri}$ (Fig. 3B), thus providing the first evidence of a physical NlpE-CpxA interaction. We next used a previously established TEM-1 β-lactamase fragment complementation assay (33). In this assay, two potentially interacting proteins are fused to two different fragments of the TEM-1 β-lactamase and their interaction is quantified by measuring resistance to β-lactams. In this experiment, we used a strain lacking *cpxR* to prevent the enhanced β-lactam resistance exhibited by cells in which Cpx is turned on (16). Remarkably, we found that the coproduction of soluble NlpE and $CpxA_{peri}$, fused to two complementary fragments of TEM-1 β-lactamase, in the periplasm substantially increased (by ≥4 log units) resistance to ampicillin (Fig. 3C). Production of NlpE or $CpxA_{peri}$ alone, fused to one of the two TEM-1 β-lactamase fragments, as well as coproduction of the noncognate lipoprotein-sensor kinase pairs NlpE and $RcsC_{peri}$ or RcsF and $CpxA_{peri}$, had no major impact (Fig. 3C). Finally, we found that overexpression of $cpxA_{peri}$ reduced the activation of Cpx that is normally observed in cells overexpressing *nlpE* (Fig. 3D), which suggests that the periplasmic domain of CpxA titrates NlpE away from the native, full-length CpxA, thus preventing Cpx activation. Together, these results provide evidence that NlpE interacts with the periplasmic domain of CpxA, which suggests that this interaction serves as a molecular signal triggering Cpx. Interestingly, similar results were obtained when the pulldown and titration assays described above were carried out with $NlpE_{Nterm}$ instead of full-length NlpE (Fig. 3B to D), thus confirming the important role played by this domain in Cpx activation.

NlpE triggers Cpx when oxidative protein folding is impaired. Because the N-terminal domain of NlpE was sufficient for Cpx activation and for physical interaction with CpxA, we wondered what the role of the C-terminal domain could possibly be.

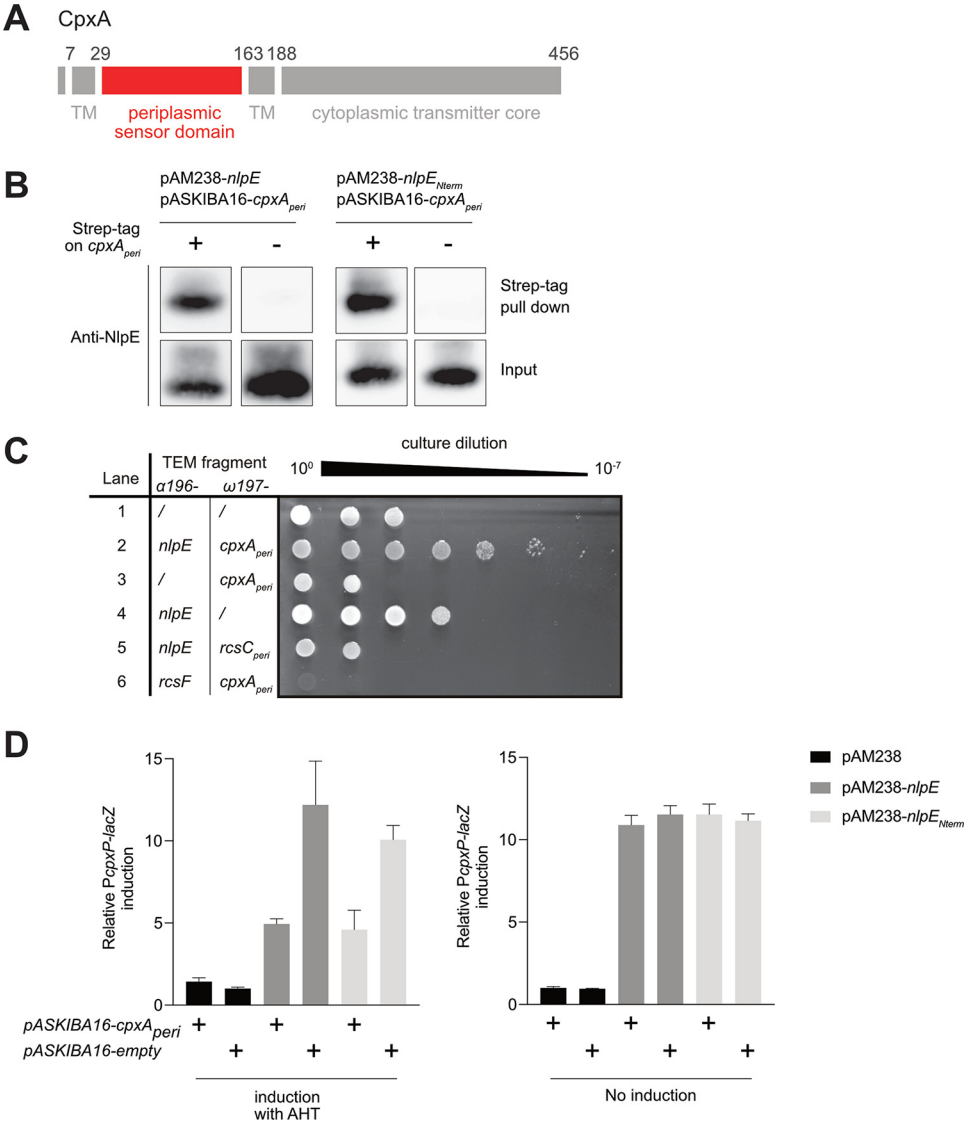

FIG 3 NlpE physically interacts with CpxA through its N-terminal domain. (A) A representative schematic of CpxA (adapted from reference 49) is shown. CpxA contains a large periplasmic sensor domain (depicted in red and determined according to reference 49 from residue 29 to 163 [inclusive]) and a cytoplasmic transmitter core. TM, transmembrane region. (B) NlpE is pulled down with CpxA. Left, expression of $cpxA_{peri}$ encoding the periplasmic domain of CpxA (as shown in panel A), fused (AD112) or not fused (AD121) to a N-terminal Strep-tag, was induced for 40 min from a pASKIBA-16 plasmid in cells overexpressing *nlpE* from the pAM238 plasmid. Right, the same procedure was performed but with cells overexpressing $nlpE_{Nterm}$ from the pAM238 plasmid, instead of the full-length *nlpE*, along with the expression of $cpxA_{peri}$ tagged with Strep-tag (AD165) or untagged $cpxA_{peri}$ (AD166) from the pASKIBA-16 plasmid. Total cell extracts were then purified on Strep-Tactin–Sepharose resin, and the input and elution (Strep-tag pulldown) fractions were analyzed by Western blotting using an anti-NlpE antibody. (C) A TEM β-lactamase complementation assay confirms *in vivo* physical interaction. Serial dilution and spotting of *cpxR* null cells carrying a pCDFDuet plasmid for the expression of the $\omega 197$ fragment and the $\alpha 196$ fragment of the TEM β-lactamase, fused or not fused to $cpxA_{peri}$, *nlpE* (soluble, without the signal sequence), $rcsC_{peri}$ (periplasmic domain of RcsC, determined according to reference 50), and/or *rcsF* (soluble, without the signal sequence), as indicated. Lane 1, AD155; lane 2, AD159; lane 3, AD160; lane 4, AD161; lane 5, AD191; lane 6, AD192. Negative controls for interaction are shown in lanes 1, 3, 4, 5, and 6. Shown is a representative image of three biological replicates. We do not know why cells became slightly more resistant in lane 4 or more sensitive in lanes 2, 5, and 6. Expression of both *nlpE* and $cpxA_{peri}$ constructs (lane 2) increased ampicillin resistance by $\geq$4 log units, compared to the *nlpE* fusion alone, indicating physical interaction. (D) Overproduced periplasmic domain of CpxA titrates NlpE or $NlpE_{Nterm}$ away from the native, full-length CpxA, preventing Cpx activation. β-Galactosidase activity from P*cpxP-lacZ* was measured with (left) or without (right) AHT induction of $cpxA_{peri}$ expression from the pASKIBA-16 plasmid, in wild-type cells overexpressing *nlpE* (AD121) or $nlpE_{Nterm}$ (AD166) or carrying the empty pAM238 vector (AD200). The same activity was measured in cells carrying the empty pASKIBA-16 plasmid (AD162, AD168, and AD201, respectively). All values were normalized to the average activity obtained for strain AD201. Bars represent the averages of normalized values from at least three independent clones. Error bars indicate standard deviations.

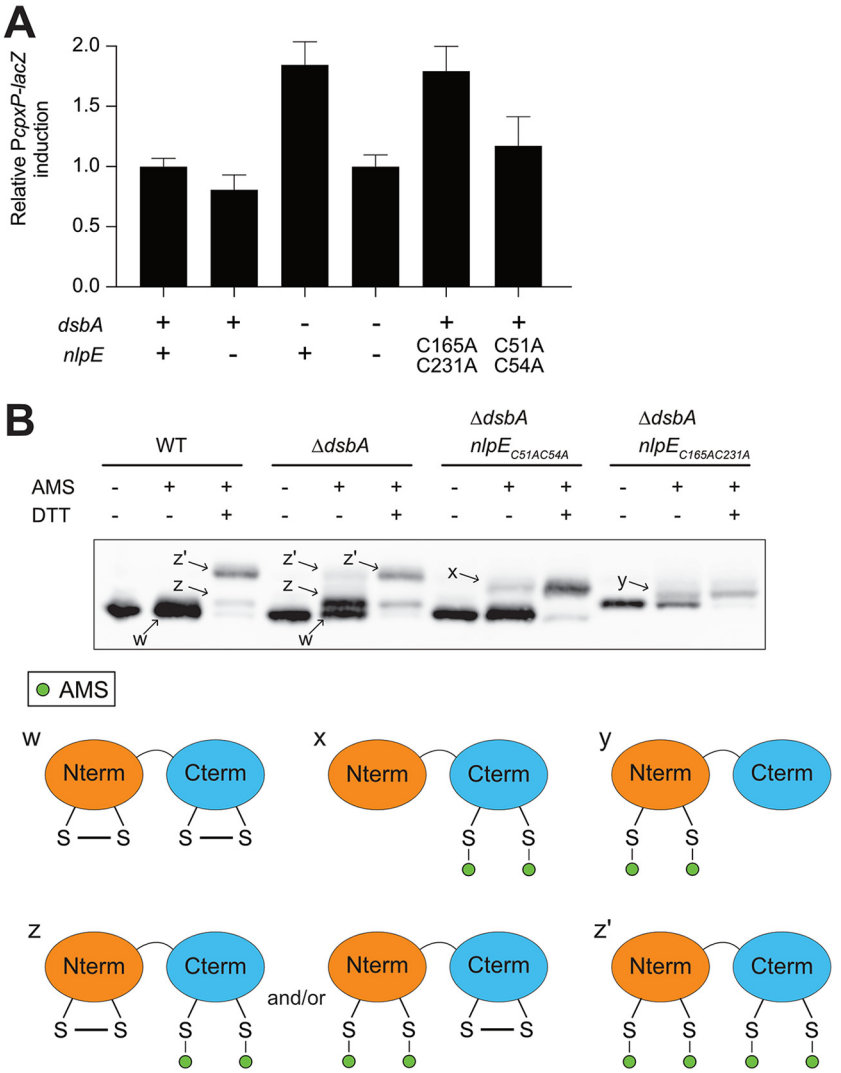

FIG 4 NlpE senses oxidative folding defects in the periplasm. (A) The oxidoreductive state of NlpE modulates Cpx activity. β-Galactosidase activity from P*cpxP-lacZ* was measured in wild-type (GL43), *nlpE*::*kanR* (GL44), Δ*dsbA* (GL64), Δ*dsbA nlpE*::*kanR* (GL65), *nlpE*::$nlpE_{C165A/C231A}$ (GL375), and *nlpE*::$nlpE_{C51A/C54A}$ (GL252) cells. All values were normalized to the average activity obtained for GL43. Bars represent the averages of normalized values for at least three independent clones. Error bars indicate standard deviations. (B) Oxidative folding defects cause reduction of the disulfide bond in the C-terminal and N-terminal domains of NlpE. Western blotting using antibody raised against NlpE shows the NlpE migration profiles for wild-type (GL43), Δ*dsbA* (GL64), Δ*dsbA nlpE*::$nlpE_{C51A/C54A}$ (GL229), and Δ*dsbA nlpE*::$nlpE_{C165A/C231A}$ (GL372) cells. Samples were either not treated, treated with AMS (alkylated control), or treated with AMS and DTT (fully reduced alkylated control) as indicated. The potential redox states corresponding to the different bands are schematized at the bottom.

NlpE contains four cysteines that form two disulfide bonds, one in each domain of the protein (Fig. 2A). DsbA is the major oxidoreductase in the periplasm of *E. coli*, being responsible for oxidizing cysteines and forming disulfide bonds (34). Since *dsbA* is a member of the Cpx regulon (35, 36), we considered the possibility that there is a functional relationship between NlpE and DsbA. To test this, we investigated the impact of *dsbA* deletion on Cpx activity. As shown in Fig. 4A, we found that deletion of *dsbA* induced Cpx ~2-fold and this induction was NlpE dependent (Fig. 4A). Interestingly, expression of a NlpE mutant lacking the C-terminal disulfide ($nlpE_{C165AC231A}$) from the native *nlpE* locus caused similar Cpx activation in wild-type cells (Fig. 4A), thus recapitulating the activation observed when the wild-type protein was expressed in the Δ*dsbA* mutant. In contrast, mutation of the N-terminal cysteines ($nlpE_{C51AC54A}$) did not

have a substantial impact on Cpx activity (see Discussion). Together, these results are consistent with the idea that NlpE activates Cpx when the C-terminal disulfide does not form.

NlpE is a DsbA substrate. To investigate the relationship between DsbA and NlpE further, we determined the *in vivo* redox state of NlpE cysteines in wild-type and Δ*dsbA* cells. To that end, we used an alkylation assay in which 4-acetamido-4′-maleimidylstilbene-2,2′-disulfonic acid (AMS), a 500-Da maleimide-based molecule, covalently modifies reduced cysteine residues; whereas oxidized proteins migrate with the expected size on SDS-PAGE, reduced proteins migrate more slowly and are shifted further toward higher molecular weights following AMS treatment (37). Treatment with AMS did not change the migration of NlpE when the protein was expressed in wild-type cells, indicating that the protein was fully oxidized. As expected, when NlpE was incubated with the reducing agent dithiothreitol (DTT) prior to modification with AMS, it migrated with a higher molecular weight (labeled z′ in Fig. 4B), corresponding to the fully reduced protein. A less abundant species (labeled z in Fig. 4B) could also be observed in the DTT-reduced sample; because it migrated faster than fully reduced NlpE, we concluded that it was a partially reduced protein still containing one disulfide bond. These experiments were then repeated in cells lacking DsbA. Although a substantial fraction of NlpE molecules migrated with the size corresponding to the fully oxidized protein (w), the same two species with slower mobility (z and z′) were detected, even without DTT treatment. These results indicated that, in the absence of DsbA, the oxidative folding of NlpE is perturbed, thus confirming that NlpE is a DsbA substrate. In addition, we observed that the partially reduced species (z) was predominant, which indicated that one of the two NlpE disulfides was more dependent on DsbA than the other.

Finally, to identify the disulfide that was still present in the partially reduced species (z), we repeated the AMS-trapping experiments in Δ*dsbA* cells expressing either $NlpE_{C51AC54A}$ or $NlpE_{C165A/C231A}$. Remarkably, $NlpE_{C165A/C231A}$ (in which only the N-terminal cysteine pair remains) was only moderately shifted following treatment with AMS, whereas the mobility of $NlpE_{C51AC54A}$ (which harbors cysteines only in the C-terminal domain) was more substantially decreased. We concluded from these experiments that the intermediate species (z) corresponded to NlpE in which the N-terminal cysteine residues are reduced. Thus, although the redox states of both pairs of cysteine residues are modified when DsbA is absent, the N-terminal cysteines appear to be particularly dependent on DsbA for oxidation to a disulfide *in vivo*.

DISCUSSION

The physiological connection between NlpE and Cpx is reinforced. It has long been known that, when overproduced, the lipoprotein NlpE activates Cpx (13), a property that turned NlpE into a useful tool to investigate the Cpx system and the resulting stress response (8). However, because overexpression of lipoproteins other than NlpE was shown to activate the synthesis of *degP* (19), a gene controlled only in part by Cpx (38), the specificity of the NlpE-Cpx relationship had remained unclear.

Here, by monitoring the activity of the *cpxP* promoter, which is specific to Cpx, unlike the promoter of *degP* (9, 10), we established that triggering of this system was dependent on the presence of NlpE under the conditions that were tested, i.e., when a dominant negative mutant of $LolA_{I93C/F140C}$ was produced in the periplasm (Fig. 1B), during treatment with globomycin (Fig. 1C), or when *dsbA* was deleted (Fig. 4A). Furthermore, in these experiments Cpx activation does not require the overproduction of NlpE, which strengthens the functional link between this lipoprotein and Cpx. Thus, our results further establish NlpE as a bona fide component of the Cpx system.

NlpE is a sensor for lipoprotein sorting defects. Two functions have been put forward for NlpE in *E. coli* to date. First, it has been reported that NlpE triggers Cpx in response to the attachment of *E. coli* to abiotic surfaces (14). Although this effect has also been shown in enterohemorrhagic *E. coli* (15), it has been disputed by a recent publication (39), and more work is needed to clarify the role of NlpE in this process.

Second, NlpE has been proposed to serve as a proxy to monitor lipoprotein trafficking to the OM and to induce Cpx when this process is perturbed (18). This second function was put forward because deletion of *nlpE* or *cpxR* decreased the survival of a LolB-depleted strain, in which lipoproteins were not efficiently transported to the OM. Note that these experiments were carried out using mutant cells also lacking RcsF and the abundant OM lipoprotein Lpp, which are toxic if accumulated in the IM (18). Experiments demonstrating unambiguously that NlpE turns on Cpx under conditions of impaired lipoprotein sorting were missing. Our results here provide direct experimental support to this idea (Fig. 1B and C). The finding that NlpE is less required for Cpx activation during long (>1-h) treatments with globomycin (Fig. 1C) is not unexpected, since this drug, which acts upstream of the lipoprotein sorting machinery, could cause broader defects at the IM, beside lipoprotein mislocalization.

In addition, while it was known that the expression of $lolA_{I93C/F140C}$ induced both the Cpx and Rcs responses, with the latter requiring the presence of RcsF (26, 27), it was thought that the Rcs response was more important to deal with defective lipoprotein sorting, because $LolA_{I93C/F140C}$ leads to the Rcs-dependent induction of *lolA* expression (27, 40). Strikingly, we found that NlpE but not RcsF contributed to increase fitness when lipoprotein trafficking was impaired (Fig. 1D), thus implying that Cpx plays a particularly important role in helping cells to cope with lipoprotein maturation problems, in agreement with other recent findings (18).

NlpE senses problems in oxidative protein folding. Oxidative folding is a required step in the maturation process for many periplasmic proteins (4). We show here that the absence of DsbA, the protein that introduces disulfide bonds in periplasmic proteins of *E. coli*, activates the Cpx system and this activation is entirely dependent on the presence of NlpE (Fig. 4A). In addition, our data suggest that NlpE turns on Cpx when the C-terminal domain does not contain a disulfide bond (Fig. 4A), thus suggesting that C-terminal cysteine residues function as a molecular sensor for redox perturbations. The molecular mechanism by which the lack of disulfide formation in NlpE causes this protein to induce Cpx remains to be determined, however. It is possible that failure to form the C-terminal disulfide alters the conformation of the C-terminal domain, with misfolding serving here as a molecular signal for Cpx activation. Alternatively, it is tempting to hypothesize that, when the C terminus of NlpE does not oxidatively fold, the export of NlpE to the OM is perturbed, causing retention of NlpE in the IM and Cpx activation (see below). Further studies will be needed to test this idea and to determine whether the localization of NlpE in the envelope is exploited to signal not only lipoprotein sorting stress but also oxidative folding defects to the Cpx system. Interestingly, NlpE harbors a highly conserved CXXC motif in its N-terminal domain, which appears to be particularly dependent on DsbA for oxidation to a disulfide (Fig. 4B). Although CXXC motifs are often involved in redox functions (41), the role of this motif in NlpE has yet to be uncovered.

NlpE induces Cpx via CpxA. Auxiliary proteins often play important roles in the regulation of two-component systems (42). This is the case, for instance, for the lipoprotein RcsF, which senses most cues inducing the Rcs system (12). Understanding how these proteins regulate their cognate systems often proves to be challenging. Regarding RcsF, although recent work shed light on the role played by OM β-barrel proteins in the occlusion of RcsF from its downstream Rcs partner under normal conditions (21, 40, 43), details of the molecular mechanism remain to be discovered. While some studies suggested a possible mechanism by which the periplasmic protein CpxP prevents signaling in nonstressed cells (44, 45), the mechanism of action of NlpE in the Cpx system remained shrouded in mystery. By showing that NlpE physically interacts with CpxA *in vivo* (Fig. 3), the results obtained here provide a first important insight into the mechanism of Cpx activation by NlpE.

It was proposed previously that conformational changes in the N-terminal domain of NlpE under stress, caused, for instance, by the lack of disulfide bond formation in this domain, could allow the C-terminal domain to reach across the periplasm to interact

with its downstream partner(s), such as the periplasmic sensing domain of CpxA (29). However, our data support a role for the N-terminal domain of NlpE in interacting with CpxA and not a role for the C-terminal domain; indeed, the C-terminal domain of NlpE is dispensable for Cpx activation when NlpE is mislocalized at the IM (Fig. 2B) and the N-terminal domain alone is sufficient to interact with $CpxA_{peri}$ (Fig. 3B and D). Furthermore, it seems unlikely that the OM-anchored N-terminal domain could reach across the periplasm to form a complex with CpxA. For these reasons, we favor an alternative hypothesis in which the targeting of NlpE to the OM prevents its N-terminal domain from interacting with CpxA under normal conditions, whereas NlpE accumulation at the IM, such as when lipoprotein trafficking is defective, allows direct contact with CpxA. The existence of additional partners in complex with NlpE and CpxA cannot be excluded at this stage, and future studies will be needed to elucidate how the N-terminal domain of NlpE talks to the Cpx sensor kinase.

Conclusions. We show that the Cpx stress response system allows *E. coli* cells to sense when the journey of lipoproteins from the IM to the OM is impaired and when the formation of disulfide bonds is perturbed, two important biogenesis processes in the envelope. Moreover, our work shows that, under these two stress conditions, the two-domain OM lipoprotein NlpE specifically triggers Cpx, which provides crucial additional support to the idea that NlpE is a bona fide member of the Cpx system. NlpE dissection led to the findings that its N-terminal domain turns on Cpx via interaction with the sensor kinase CpxA and that two cysteine residues in its C-terminal domain work as a redox sensor when oxidative folding is hindered. We conclude that Cpx uses the localization and redox status of NlpE as proxies to monitor lipoprotein sorting and oxidative folding in the *E. coli* envelope.

MATERIALS AND METHODS

Bacterial strains, media, and plasmids. All strains and plasmids, as well as construction methods, can be found in Table S1 in the supplemental material. Primers are listed in Table S2. Cells were grown in LB medium at 37°C except when indicated otherwise. To avoid any effect of Cpx activation that starts in late exponential phase (9, 46), most experiments were performed with cultures grown to early log or mid-log phase (optical density at 600 nm [OD_{600}] of ≤0.6), usually after diluting an overnight inoculum 1:1,000 (never less than 1:500) in order to ensure exit of stationary phase. Antibiotics were used for plasmid maintenance when appropriate, at the following concentrations: ampicillin, 200 μg/ml; spectinomycin, 50 μg/ml; kanamycin, 50 μg/ml; chloramphenicol, 20 μg/ml.

β-Galactosidase assays. β-Galactosidase activity was assayed as described (47) or using a slightly modified protocol that used the V_{max} of the β-galactosidase reaction as a readout. Briefly, the OD_{600} of the sample was measured, and then 5 μl was transferred to 20 μl of solution A (47) in a 96-well plate. Solution B (47) was then added and β-galactosidase activity was analyzed by kinetic measurement of the OD_{420} in a Synergy H1 microplate reader (Biotek). V_{max} was determined using Gen5 software and normalized to the OD_{600}. For time-course experiments, cells were grown in LB medium with appropriate antibiotics for 150 min, at which point the cells were induced by the addition of 0.2% L-arabinose or treated with 10 μM globomycin (Sigma). β-Galactosidase activity was measured periodically. Graphs were prepared using Prism 7 (GraphPad Software, Inc.).

Fitness spot titer assay. Single colonies were used to inoculate overnight cultures, which were diluted 1:500 in 5 ml LB medium with antibiotics when appropriate for plasmid maintenance. The cells were grown to an OD_{600} of 0.2 and then either serially diluted 5-fold in a 96-well plate and spotted on LB agar supplemented with chloramphenicol (20 μg/ml) or induced by the addition of 0.2% L-arabinose and then spotted in the same manner after 1.5 and 4.5 h of induction. The plates were then imaged using a GE ImageQuant LAS4000 camera (GE Healthcare Life Sciences).

Pulldown assay. Single colonies were used to inoculate overnight cultures, which were diluted 1:500 in 400 ml LB medium containing ampicillin and spectinomycin for plasmid maintenance. When the OD_{600} reached 0.2, the expression of CpxA, with or without a Strep-tag, was induced with the addition of 50 ng/ml anhydrotetracycline (AHT). After 40 min of expression, the cells were pelleted, resuspended in 10 ml of buffer W (100 mM Tris-HCl [pH 8.0], 150 mM NaCl), and lysed with a French press. The lysate was applied to 500 μl of Strep-Tactin–Sepharose resin (IBA Lifesciences). The resin was washed according to the manufacturer's recommendations, and the protein was eluted with buffer W supplemented with 2.5 mM *d*-desthiobiotin. The elution fractions were mixed with 5× nonreducing Laemmli buffer in a 5:1 ratio and boiled before Western blotting.

TEM-1 β-lactamase complementation assay. The assay was performed as described previously (48), with the following modifications. Cells were grown to stationary phase in LB medium supplemented with spectinomycin (50 μg/ml). They were then serially diluted (10-fold) and plated on LB agar plates supplemented with 0.01 mM isopropyl-β-D-1-thiogalactopyranoside (IPTG) and 20 μg/ml ampicillin. The plates were imaged after overnight incubation at 37°C, using a GE ImageQuant LAS4000 camera (GE Healthcare Life Sciences).

CpxA titration assay. Single colonies were used to inoculate overnight cultures, which were diluted 1:500 in 5 ml LB medium. When the OD_{600} reached 0.2, the cells were induced with the addition of 50 ng/ml AHT for 1 h, after which β-galactosidase activity was measured as described above. To keep the cells in the exponential growth phase, cultures were diluted 4-fold in fresh medium during induction.

Western blotting. Proteins from exponentially growing cultures were precipitated with trichloroacetic acid as described previously (37), solubilized in 1× nonreducing Laemmli buffer (48) (the volume for each sample was adapted to normalize all samples according to the OD_{600}), and boiled before being loaded on precast 12% NuPAGE Bis-Tris gels (Life Technologies). Western blotting was performed using standard procedures, with primary antibodies directed against NlpE, RcsF, Lpp, and DsbD (rabbit sera; CER Group, Marloie, Belgium), followed by a horseradish peroxidase (HRP)-conjugated anti-rabbit IgG secondary antibody (Sigma). Chemiluminescence signals were imaged by using a GE ImageQuant LAS4000 camera (GE Healthcare Life Sciences) or by using X-ray films (for the RcsF blots in Fig. S1D).

AMS alkylation assay. The *in vivo* redox state of NlpE was assessed using AMS trapping experiments, as described previously (37). Samples were loaded onto 12% NuPAGE Bis-Tris gels (Life Technologies) under denaturing conditions. After electrophoresis, the proteins were transferred to a nitrocellulose membrane and probed with an anti-NlpE antibody.

Cell fractionation. Cell fractionation was performed as described previously (16).

SUPPLEMENTAL MATERIAL

Supplemental material for this article may be found at https://doi.org/10.1128/JB.00611-18.

SUPPLEMENTAL FILE 1, PDF file, 0.7 MB.

ACKNOWLEDGMENTS

We are grateful to Seung-Hyun Cho for kindly providing the membrane localization data for RcsF and $RcsF_{IM}$ shown in Fig. S1D in the supplemental material, to Camille Goemans, Pauline Leverrier, and Alexandra Gennaris for critical reading of the manuscript, and to all members of the Collet laboratory for insightful discussions. We thank Diarmaid Hughes (Uppsala University) for strain CH1990, Shu Quan (East China University of Science and Technology) for the kind gift of pCDFDuet-based plasmids used for the TEM β-lactamase fragment assay (as indicated in Table S1), Thomas Silhavy (Princeton University) for the kind gift of strain PAD282, and Joanna Szewczyk and Pauline Leverrier (Collet laboratory) for the construction of strains and plasmids, as indicated in Table S1.

We declare that we have no conflicts of interest.

All experiments were performed and analyzed by A.D. and G.L.; J.-F.C. and G.L. designed and supervised the research; and A.D., G.L., and J.-F.C. wrote the manuscript.

A.D. is a research fellow of the F.R.S.-FNRS, and G.L. is a research associate of the F.R.S.-FNRS; J.-F.C. was a research director of the F.R.S.-FNRS and is an investigator of the FRFS-WELBIO. This work was funded by the WELBIO and a Crédit de Recherche grant from the F.R.S.-FNRS (STRESS, to J.-F.C.).

The funders had no role in study design, data collection and interpretation, or the decision to submit the work for publication.

REFERENCES

1. Silhavy TJ, Kahne D, Walker S. 2010. The bacterial cell envelope. Cold Spring Harb Perspect Biol 2:a000414. https://doi.org/10.1101/cshperspect.a000414.
2. Typas A, Banzhaf M, Gross CA, Vollmer W. 2011. From the regulation of peptidoglycan synthesis to bacterial growth and morphology. Nat Rev Microbiol 10:123–136. https://doi.org/10.1038/nrmicro2677.
3. Szewczyk J, Collet JF. 2016. The journey of lipoproteins through the cell: one birthplace, multiple destinations. Adv Microb Physiol 69:1–50. https://doi.org/10.1016/bs.ampbs.2016.07.003.
4. Goemans C, Denoncin K, Collet J-F. 2014. Folding mechanisms of periplasmic proteins. Biochim Biophys Acta 1843:1517–1528. https://doi.org/10.1016/j.bbamcr.2013.10.014.
5. Okuda S, Sherman DJ, Silhavy TJ, Ruiz N, Kahne D. 2016. Lipopolysaccharide transport and assembly at the outer membrane: the PEZ model. Nat Rev Microbiol 14:337–345. https://doi.org/10.1038/nrmicro.2016.25.
6. Grabowicz M, Silhavy TJ. 2017. Envelope stress responses: an interconnected safety net. Trends Biochem Sci 42:232–242. https://doi.org/10.1016/j.tibs.2016.10.002.
7. Rowley G, Spector M, Kormanec J, Roberts M. 2006. Pushing the envelope: extracytoplasmic stress responses in bacterial pathogens. Nat Rev Microbiol 4:383–394. https://doi.org/10.1038/nrmicro1394.
8. Raivio TL. 2014. Everything old is new again: an update on current research on the Cpx envelope stress response. Biochim Biophys Acta 1843:1529–1541. https://doi.org/10.1016/j.bbamcr.2013.10.018.
9. DiGiuseppe PA, Silhavy TJ. 2003. Signal detection and target gene induction by the CpxRA two-component system. J Bacteriol 185:2432–2440. https://doi.org/10.1128/JB.185.8.2432-2440.2003.
10. Price NL, Raivio TL. 2009. Characterization of the Cpx regulon in *Escherichia coli* strain MC4100. J Bacteriol 191:1798–1815. https://doi.org/10.1128/JB.00798-08.
11. Raivio TL, Leblanc SKD, Price NL. 2013. The *Escherichia coli* Cpx envelope stress response regulates genes of diverse function that impact antibiotic resistance and membrane integrity. J Bacteriol 195:2755–2767. https://doi.org/10.1128/JB.00105-13.
12. Laloux G, Collet J-F. 2017. Major Tom to ground control: how lipoproteins communicate extracytoplasmic stress to the decision center of the cell. J Bacteriol 199:e00216-17. https://doi.org/10.1128/JB.00216-17.

13. Snyder WB, Davis LJ, Danese PN, Cosma CL, Silhavy TJ. 1995. Overproduction of NlpE, a new outer membrane lipoprotein, suppresses the toxicity of periplasmic LacZ by activation of the Cpx signal transduction pathway. J Bacteriol 177:4216–4223. https://doi.org/10.1128/jb.177.15.4216-4223.1995.
14. Otto K, Silhavy TJ. 2002. Surface sensing and adhesion of *Escherichia coli* controlled by the Cpx-signaling pathway. Proc Natl Acad Sci U S A 99:2287–2292. https://doi.org/10.1073/pnas.042521699.
15. Shimizu T, Ichimura K, Noda M. 2016. The surface sensor NlpE of enterohemorrhagic *Escherichia coli* contributes to regulation of the type III secretion system and flagella by the Cpx response to adhesion. Infect Immun 84:537–549. https://doi.org/10.1128/IAI.00881-15.
16. Delhaye A, Collet J-F, Laloux G. 2016. Fine-tuning of the Cpx envelope stress response is required for cell wall homeostasis in *Escherichia coli*. mBio 7:e00047-16. https://doi.org/10.1128/mBio.00047-16.
17. Wall E, Majdalani N, Gottesman S. 2018. The complex Rcs regulatory cascade. Annu Rev Microbiol 72:111–139. https://doi.org/10.1146/annurev-micro-090817-062640.
18. Grabowicz M, Silhavy TJ. 2017. Redefining the essential trafficking pathway for outer membrane lipoproteins. Proc Natl Acad Sci U S A 114:4769–4774. https://doi.org/10.1073/pnas.1702248114.
19. Miyadai H, Tanaka-Masuda K, Matsuyama S-I, Tokuda H. 2004. Effects of lipoprotein overproduction on the induction of DegP (HtrA) involved in quality control in the *Escherichia coli* periplasm. J Biol Chem 279:39807–39813. https://doi.org/10.1074/jbc.M406390200.
20. Farris C, Sanowar S, Bader MW, Pfuetzner R, Miller SI. 2010. Antimicrobial peptides activate the Rcs regulon through the outer membrane lipoprotein RcsF. J Bacteriol 192:4894–4903. https://doi.org/10.1128/JB.00505-10.
21. Konovalova A, Mitchell AM, Silhavy TJ. 2016. A lipoprotein/β-barrel complex monitors lipopolysaccharide integrity transducing information across the outer membrane. Elife 5:e15276. https://doi.org/10.7554/eLife.15276.
22. 22.Okuda S, Tokuda H. 2011. Lipoprotein sorting in bacteria. Annu Rev Microbiol 65:239–259. https://doi.org/10.1146/annurev-micro-090110-102859.
23. Yakushi T, Masuda K, Narita S, Matsuyama S, Tokuda H. 2000. A new ABC transporter mediating the detachment of lipid-modified proteins from membranes. Nat Cell Biol 2:212–218. https://doi.org/10.1038/35008635.
24. Tajima T, Yokota N, Matsuyama S, Tokuda H. 1998. Genetic analyses of the in vivo function of LolA, a periplasmic chaperone involved in the outer membrane localization of *Escherichia coli* lipoproteins. FEBS Lett 439:51–54. https://doi.org/10.1016/S0014-5793(98)01334-9.
25. Matsuyama SI, Yokota N, Tokuda H. 1997. A novel outer membrane lipoprotein, LolB (HemM), involved in the LolA (p20)-dependent localization of lipoproteins to the outer membrane of *Escherichia coli*. EMBO J 16:6947–6955. https://doi.org/10.1093/emboj/16.23.6947.
26. Tao K, Watanabe S, Narita S-I, Tokuda H. 2010. A periplasmic LolA derivative with a lethal disulfide bond activates the Cpx stress response system. J Bacteriol 192:5657–5662. https://doi.org/10.1128/JB.00821-10.
27. Tao K, Narita S-I, Tokuda H. 2012. Defective lipoprotein sorting induces *lolA* expression through the Rcs stress response phosphorelay system. J Bacteriol 194:3643–3650. https://doi.org/10.1128/JB.00553-12.
28. Vogeley L, El Arnaout T, Bailey J, Stansfeld PJ, Boland C, Caffrey M. 2016. Structural basis of lipoprotein signal peptidase II action and inhibition by the antibiotic globomycin. Science 351:876–880. https://doi.org/10.1126/science.aad3747.
29. Hirano Y, Hossain MM, Takeda K, Tokuda H, Miki K. 2007. Structural studies of the Cpx pathway activator NlpE on the outer membrane of *Escherichia coli*. Structure 15:963–976. https://doi.org/10.1016/j.str.2007.06.014.
30. Campanacci V, Bishop RE, Blangy S, Tegoni M, Cambillau C. 2006. The membrane bound bacterial lipocalin Blc is a functional dimer with binding preference for lysophospholipids. FEBS Lett 580:4877–4883. https://doi.org/10.1016/j.febslet.2006.07.086.
31. Ginalski K, Kinch L, Rychlewski L, Grishin NV. 2004. BOF: a novel family of bacterial OB-fold proteins. FEBS Lett 567:297–301. https://doi.org/10.1016/j.febslet.2004.04.086.
32. Raivio TL, Silhavy TJ. 1997. Transduction of envelope stress in *Escherichia coli* by the Cpx two-component system. J Bacteriol 179:7724–7733. https://doi.org/10.1128/jb.179.24.7724-7733.1997.
33. Galarneau A, Primeau M, Trudeau L-E, Michnick SW. 2002. β-Lactamase protein fragment complementation assays as in vivo and in vitro sensors of protein-protein interactions. Nat Biotechnol 20:619–622. https://doi.org/10.1038/nbt0602-619.
34. Bardwell JC, McGovern K, Beckwith J. 1991. Identification of a protein required for disulfide bond formation in vivo. Cell 67:581–589. https://doi.org/10.1016/0092-8674(91)90532-4.
35. Pogliano J, Lynch AS, Belin D, Lin EC, Beckwith J. 1997. Regulation of *Escherichia coli* cell envelope proteins involved in protein folding and degradation by the Cpx two-component system. Genes Dev 11:1169–1182. https://doi.org/10.1101/gad.11.9.1169.
36. Danese PN, Silhavy TJ. 1997. The sigma(E) and the Cpx signal transduction systems control the synthesis of periplasmic protein-folding enzymes in *Escherichia coli*. Genes Dev 11:1183–1193. https://doi.org/10.1101/gad.11.9.1183.
37. Denoncin K, Nicolaes V, Cho S-H, Leverrier P, Collet J-F. 2013. Protein disulfide bond formation in the periplasm: determination of the in vivo redox state of cysteine residues. Methods Mol Biol 966:325–336. https://doi.org/10.1007/978-1-62703-245-2_20.
38. Danese PN, Snyder WB, Cosma CL, Davis LJ, Silhavy TJ. 1995. The Cpx two-component signal transduction pathway of *Escherichia coli* regulates transcription of the gene specifying the stress-inducible periplasmic protease, DegP. Genes Dev 9:387–398. https://doi.org/10.1101/gad.9.4.387.
39. Kimkes TEP, Heinemann M. 2018. Reassessing the role of the *Escherichia coli* CpxAR system in sensing surface contact. PLoS One 13:e0207181. https://doi.org/10.1371/journal.pone.0207181.
40. Cho S-H, Szewczyk J, Pesavento C, Zietek M, Banzhaf M, Roszczenko P, Asmar A, Laloux G, Hov A-K, Leverrier P, Van der Henst C, Vertommen D, Typas A, Collet J-F. 2014. Detecting envelope stress by monitoring β-barrel assembly. Cell 159:1652–1664. https://doi.org/10.1016/j.cell.2014.11.045.
41. Quan S, Schneider I, Pan J, Von Hacht A, Bardwell J. 2007. The CXXC motif is more than a redox rheostat. J Biol Chem 282:28823–28833. https://doi.org/10.1074/jbc.M705291200.
42. Capra EJ, Laub MT. 2012. Evolution of two-component signal transduction systems. Annu Rev Microbiol 66:325–347. https://doi.org/10.1146/annurev-micro-092611-150039.
43. Konovalova A, Perlman DH, Cowles CE, Silhavy TJ. 2014. Transmembrane domain of surface-exposed outer membrane lipoprotein RcsF is threaded through the lumen of β-barrel proteins. Proc Natl Acad Sci U S A 111:E4350–E4358. https://doi.org/10.1073/pnas.1417138111.
44. Zhou X, Keller R, Volkmer R, Krauss N, Scheerer P, Hunke S. 2011. Structural basis for two-component system inhibition and pilus sensing by the auxiliary CpxP protein. J Biol Chem 286:9805–9814. https://doi.org/10.1074/jbc.M110.194092.
45. Tschauner K, Hörnschemeyer P, Müller VS, Hunke S. 2014. Dynamic interaction between the CpxA sensor kinase and the periplasmic accessory protein CpxP mediates signal recognition in *E. coli*. PLoS One 9:e107383. https://doi.org/10.1371/journal.pone.0107383.
46. De Wulf P, Kwon O, Lin EC. 1999. The CpxRA signal transduction system of *Escherichia coli*: growth-related autoactivation and control of unanticipated target operons. J Bacteriol 181:6772–6778.
47. Zhang X, Bremer H. 1995. Control of the *Escherichia coli rrnB* P1 promoter strength by ppGpp. J Biol Chem 270:11181–11189. https://doi.org/10.1074/jbc.270.19.11181.
48. Bai L, He W, Li T, Yang C, Zhuang Y, Quan S. 2017. Chaperone-substrate interactions monitored via a robust TEM-1 β-lactamase fragment complementation assay. Biotechnol Lett 39:1191–1199. https://doi.org/10.1007/s10529-017-2347-9.
49. Mechaly AE, Sassoon N, Betton J-M, Alzari PM. 2014. Segmental helical motions and dynamical asymmetry modulate histidine kinase autophosphorylation. PLoS Biol 12:e1001776. https://doi.org/10.1371/journal.pbio.1001776.
50. Sato T, Takano A, Hori N, Izawa T, Eda T, Sato K, Umekawa M, Miyagawa H, Matsumoto K, Muramatsu-Fujishiro A, Matsumoto K, Matsuoka S, Hara H. 2017. Role of the inner-membrane histidine kinase RcsC and outer-membrane lipoprotein RcsF in the activation of the Rcs phosphorelay signal transduction system in *Escherichia coli*. Microbiology 163:1071–1080. https://doi.org/10.1099/mic.0.000483.